11 Reflection Polarization of Rayleigh Skylight at the Air-Water Interface

In the optical environment one of the main sources of partially linearly polarized light is that reflected from water surfaces. The reflection-polarization pattern of water surfaces is a striking cue and plays an important role in the habitat search of insects associated with water.

In this chapter a quantitative account is given of the physics of polarization of single-scattered Rayleigh skylight due to reflection from the water surface on the basis of the results of Schwind and Horváth (1993) and Horváth (1995a). The light arising from the bottom or reflected by particles suspended in water is neglected. Spectral and intensity characteristics of the skylight and the wavelength-dependence of the refractive index of water are not taken into consideration.

11.1 Reflectivity, Reflection-Polarization Ellipse, Degree and Angle of Linear Polarization of Light Reflected from the Water Surface

The amplitude reflection coefficients $\rho_{hor}(\theta_i)$ and $\rho_{ver}(\theta_i)$ versus the angle of incidence θ_i (Guenther 1990) describe how the horizontal and vertical components of the electric field vector $\underline{E}$ change after reflection from the water surface. Figure 11.1A shows $\rho_{hor}(\theta_i)$ and $\rho_{ver}(\theta_i)$ for the air-water interface. There is a sign change in ρ_{ver} at the Brewster angle $\theta_{Brewster} = 53^o$ measured from the vertical. Vertically polarized light is considerably weakened when reflected from the water surface and at the Brewster angle its intensity even falls to zero, while horizontally polarized light is much less weakened. Thus the water surface reflects vertically polarized light much less effectively than horizontally polarized light.

In general, partially linearly polarized light with an arbitrary direction of polarization can be decomposed into a horizontally and a vertically polarized component which vibrate coherently. As the horizontal component is less weakened after reflection, the plane of polarization of the sum of the components will become more horizontal, that is, the E-vector rotates after reflection towards the water surface. The sign change of ρ_{ver} at the Brewster angle has the consequence that the reflected electric field vector is exactly horizontal, if $\theta_i = \theta_{Brewster}$. If $\theta_i < \theta_{Brewster}$, the plane of polarization is also mirrored besides the rotation towards the water surface. This mirroring is caused by an additional

phase-shift of 180° of the vertically polarized component after reflection, because ρ_{ver} is then negative, which does not occur for horizontally polarized light. For $\theta_i > \theta_{Brewster}$ this phase-shift is absent, because ρ_{ver} is then positive. The dependence of the reflectivity R of the water surface on θ_i and the angle of polarization α_i of totally linearly polarized incident light is shown in Figs. 11.1B and 11.1C.

The direct sunlight, the light coming from the neutral points of the sky and the light from the heavily overcast sky are unpolarized, that is, their polarization ellipse is a circle. After reflection from the water surface this unpolarized incident light becomes partially linearly polarized with horizontal E-vector irrespective of θ_i. The change of the degree of linear polarization p of reflected light versus θ_i can be read qualitatively from the shape of the reflection-polarization ellipses in Figs. 11.2A and 11.2B, and quantitatively in Fig. 11.2C. Figure 11.2D shows the reflectivity of the water surface versus θ_i for unpolarized incident light. The horizontal dimension of the reflection-polarization ellipse increases monotonously with increasing θ_i, because $\rho_{hor}(\theta_i)$ increases monotonously and has always positive values (Fig. 11.1A). However, the vertical dimension of the reflection-polarization ellipse decreases with increasing θ_i up to the Brewster angle $\theta_{Brewster}$, then it increases with θ_i because of the sign change of $\rho_{ver}(\theta_i)$ (Fig. 11.1A). Representing the series of the reflection-polarization ellipses in three dimensions versus θ_i, the quasi-exponential increase of ρ_{ver} and ρ_{hor} for $\theta_i > \theta_{Brewster}$ results in a special trumpet-like form, which is horizontally flattened at the Brewster angle (Fig. 11.2B).

The degree of linear polarization p_r of reflected light for unpolarized incident light increases from 0% to 100% as θ_i increases from 0° to $\theta_{Brewster}$, then it decreases from 100% to 0% as θ_i increases from $\theta_{Brewster}$ to 90° (Fig. 11.2C). This change of p_r means that the shape of the reflection-polarization ellipse is circular at $\theta_i = 0°$ and $\theta_i = 90°$, and it becomes horizontally more flattened with increasing θ_i, and at the Brewster angle it is distorted to a straight horizontal line, which means that the reflected light is totally linearly polarized. Similar but opposite change occurs in the shape of the reflection-polarization ellipse when θ_i increases from $\theta_{Brewster}$ to 90° (Figs. 11.2A and 11.2B). The reflectivity of the water surface for unpolarized incident light increases quasi-exponentially with θ_i (Fig. 11.2D).

Figure 11.3 shows the reflection-polarization ellipses, p_r and α_r of light reflected from the water surface versus θ_i for partially linearly polarized incident light with $p_i = 50\%$ and four different α_i-values. Due to the sign change of $\rho_{ver}(\theta_i)$ (Fig. 11.1A), also α_r has a sign change at the Brewster angle as can be seen in the plots of $\alpha_r(\theta_i)$ in Fig. 11.3. Figures 11.4 and 11.5 show the dependence of p_r and α_r of light reflected from the water surface as functions of θ_i, α_i and p_i of the incident light.

Hence, if the incident light is partially linearly polarized, as the skylight for instance, the effects of reflection of the unpolarized and totally linearly polarized parts of the incident light can be summed. The unpolarized component is partially converted into horizontally polarized light and the totally polarized part rotates its plane of vibration towards the water surface, while in addition this plane is or is

not mirrored if the angle of incidence is smaller or larger than the Brewster angle, respectively (Figs. 11.3-11.5). The net effect is an increase in the degree of polarization and a stronger rotation of the polarization plane towards the water surface than is the case when the incident light is totally linearly polarized.

11.2 Polarization Patterns of Single-Scattered Rayleigh Skylight Reflected from the Flat Water Surface as a Function of the Solar Zenith Angle

A possible way of displaying polarization patterns is to represent the direction of polarization by the orientation of a bar, the width of which is proportional to p. Such polarization patterns of the clear single-scattering Rayleigh sky are shown in Fig. 11.6 for four solar zenith angles. Figure 11.7 shows the polarization patterns of single-scattered Rayleigh skylight reflected from the flat water surface for the same solar zenith angles. In Figs. 11.8A-D the pattern of reflectivity R of the water surface versus the solar zenith angle is seen for the single-scattered Rayleigh skylight. Figure 11.8E shows the R-pattern of the water surface for unpolarized light from a totally overcast sky.

The disadvantage of these representations of the distribution of polarization is that due to the relatively large dimensions of the bars and polarization ellipses the spatial resolution of these patterns is low. This disadavantage is eliminated in Figs. 7.6.1D,E; 7.6.2D,E and 11.9, 11.10 showing the colour-coded patterns of p and α of single-scattered Rayleigh skylight and Rayleigh skylight reflected from the water surface for different solar zenith angles. The most important features of the water-surface-reflected polarization patterns are the following:

- At or near the Brewster angle the polarization ellipses are distorted to horizontal lines tangential in circular two-dimensional representation or become horizontally very flattened, because p_r of reflected light is approximately 100%. Hence there is a characteristic, nearly totally and horizontally polarized annular Brewster zone on the water surface (Figs. 11.7, 11.9, 11.10).
- At lower solar elevations the E-vectors of reflected light are mainly horizontal towards the sun and opposite to it (Figs. 11.7C,D and 11.10C,D). Apart from the annular Brewster zone, at 90^o from the sun, the E-vectors of reflected light are mainly vertical i.e. radial in two-dimensional representation. This band, visible at the water surface and interrupted twice by the Brewster zone (Figs. 11.7C,D and 11.10C,D), is the counterpart of the maximally polarized continuous band in the clear sky at 90^o from the sun (Figs. 11.6C,D).

Comparing the R-patterns of the water surface calculated for clear skies (Figs. 11.8A-D) with the R-pattern for unpolarized light from a heavily overcast sky (Fig. 11.8E), we can establish that there is no significant difference between them and they all have quasi-cylindrical symmetry for $R > 7\%$, that is, for directions of

observations larger than 65° from the vertical. The *R*-pattern calculated for the clear sky with sun at the zenith (Fig. 11.8A) and that for unpolarized skylight (Fig. 11.8E) have exact cylindrical symmetry. As the sun nears the horizon, the contour lines of equal reflectivity become gradually elliptical being flattened perpendicularly to the solar meridian.

The two central black spots in Figs. 11.8C and 11.8D are regions of the water surface where $R < 2\%$. The water surface is clearly more transparent at these dark spots, because there is hardly any reflection-gloss. In ditches, even with slightly rippling water, these dark spots are also distinctly visible. Then the spots make the impression of being more or less triangular, that can be deduced from the shape of these spots (Figs. 11.8C and 11.8D). These dark spots can be photographed without a polarizing filter, too (see e.g. Plate 10 of Können 1985, p. 30).

11.3 Effect of Clouds on the Reflection-Polarization Pattern of the Water Surface

When the sky is partly cloudy, some regions of the celestial polarization pattern are hidden. Figure 11.11 demonstrates this situation. Here, the celestial *p*-patterns are partly covered by simulated clouds. For the sake of simplicity, the light radiated by clouds[1] is supposed to be unpolarized, so the depolarizing clouds are represented by white in Fig. 11.11.

Figure 11.12 shows the *p*-pattern of skylight reflected from the water surface as a function of the solar zenith angle for the cloudy Rayleigh skies in Fig. 11.11. Contrary to the uniformly white shade of the clouds in Fig. 11.11, the mirror clouds in Fig. 11.12 are heterogeneously grey, because the unpolarized incident cloud light becomes horizontally polarized after reflection from the water surface with *p* depending on the direction of view from the nadir as shown in Fig. 11.9E. In Fig. 11.12 the patterns of Figs. 11.9A-D are combined with the pattern of Fig. 11.9E in such a way, that in the patches of the mirror clouds the pattern of Fig. 11.9E is seen.

[1] The polarizational characteristics of clouds are diverse. There are many kinds of clouds, and the polarization of their light depends on their illumination, composition, height, density and the size of their elements. α of light from higher clouds is the same as that of the blue sky, its *p*, however, differs considerably (see Chapters 7.6 and 7.7). The maximum *p* of ice-clouds and water-clouds is not higher than about 40%. Their polarization decreases in directions closer to or further away from the sun. In water-clouds the light is strongly polarized at 90° from the sun and due to the rainbow-scattering it is most strongly polarized at about 145° from the sun, which can be as high as 60%. *p* of cloudlight is generally lower if the clouds are denser.

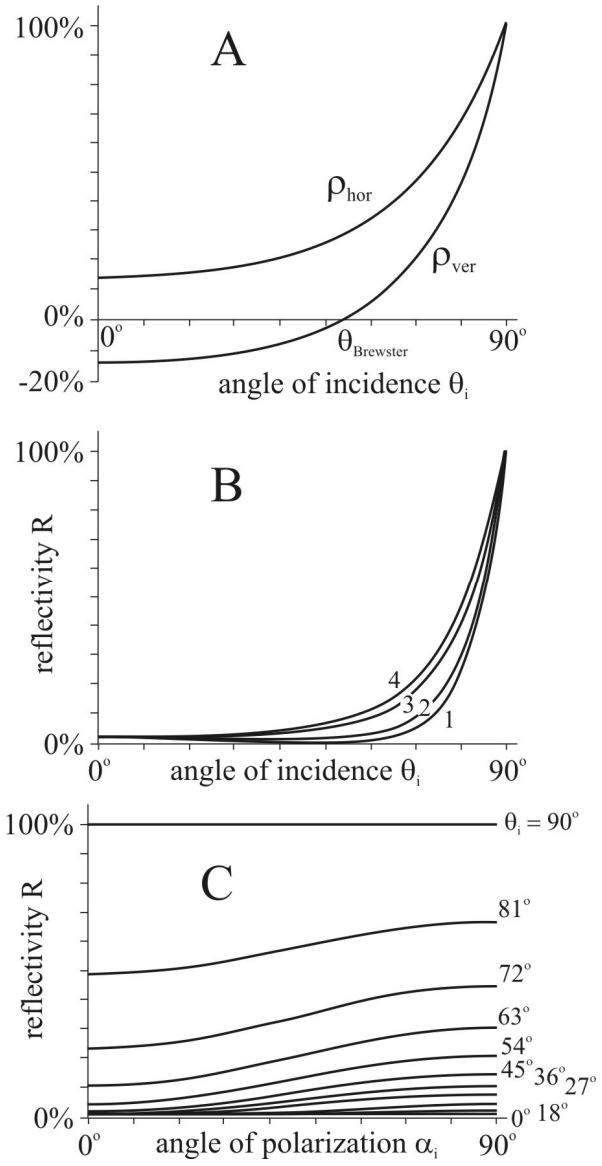

Fig. 11.1. A: Amplitude reflection coefficients ρ_{hor} and ρ_{ver} as a function of the incident angle θ_i measured from the vertical for horizontal and vertical E-vector of totally linearly polarized incident light calculated for the air-water interface with indices of refraction n_{air} = 1 and n_{water} = 1.33. B: Reflectivity $R(\theta_i)$ of the water surface for totally linearly polarized incident light with different angles of polarization α_i measured from the vertical. 1: $\alpha_i = 0^o$, 2: $\alpha_i = 30^o$, 3: $\alpha_i = 60^o$, 4: $\alpha_i = 90^o$. C: Reflectivity $R(\alpha_i)$ of the water surface for different θ_i of totally linearly polarized incident light. θ_i changes from 90° to 0° with a step of $\Delta\theta_i = 9^o$. (After Fig. 5.1 of Horváth 1993, p. 77).

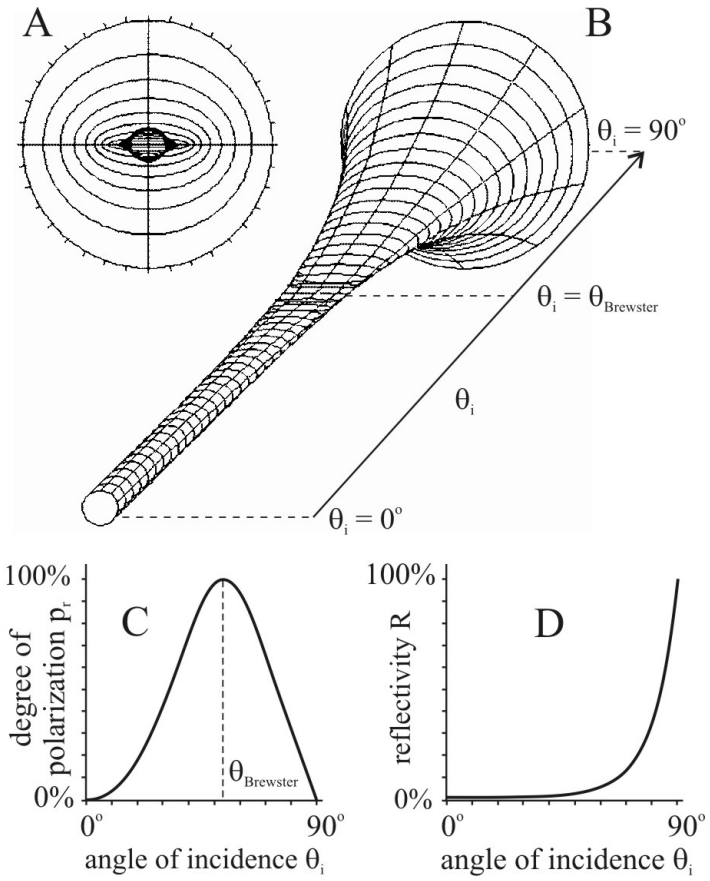

Fig. 11.2. A: Reflection-polarization ellipses calculated for the water surface for unpolarized incident light as a function of the angle of incidence θ_i measured from the vertical and increasing from the Brewster angle $\theta_{Brewster}$ to 90° in steps of $\Delta\theta_i = 6°$ from the center towards the periphery. The outermost circle with a graduation scale of 10° represents the polarization circle of the neutral incident light. B: Three-dimensional representation of the reflection-polarization ellipses versus θ_i. For $\theta_i = \theta_{Brewster} = 53°$ the reflected light is totally and horizontally polarized. C: Degree of linear polarization p_r of light reflected from the water surface versus θ_i calculated for unpolarized incident light. D: Reflectivity R of the water surface versus θ_i for unpolarized incident light. (After Fig. 5.2 of Horváth 1993, p. 78).

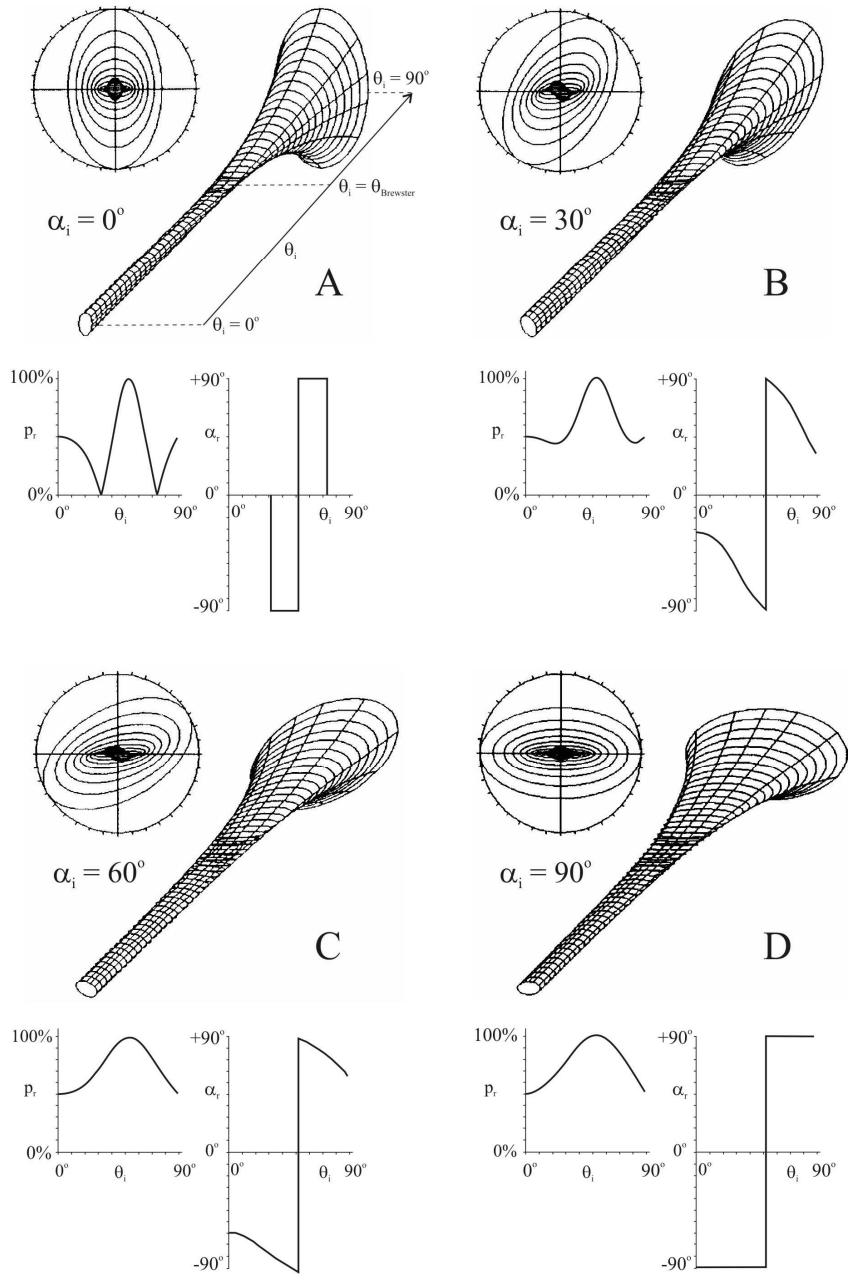

Fig. 11.3. Reflection-polarization ellipses, degree p_r and angle α_r of linear polarization of light reflected from the water surface versus the angle of incidence θ_i for partially linearly polarized incident light with p_i = 50% and four different α_i measured from the vertical. (After Fig. 5.3 of Horváth 1993, p. 80).

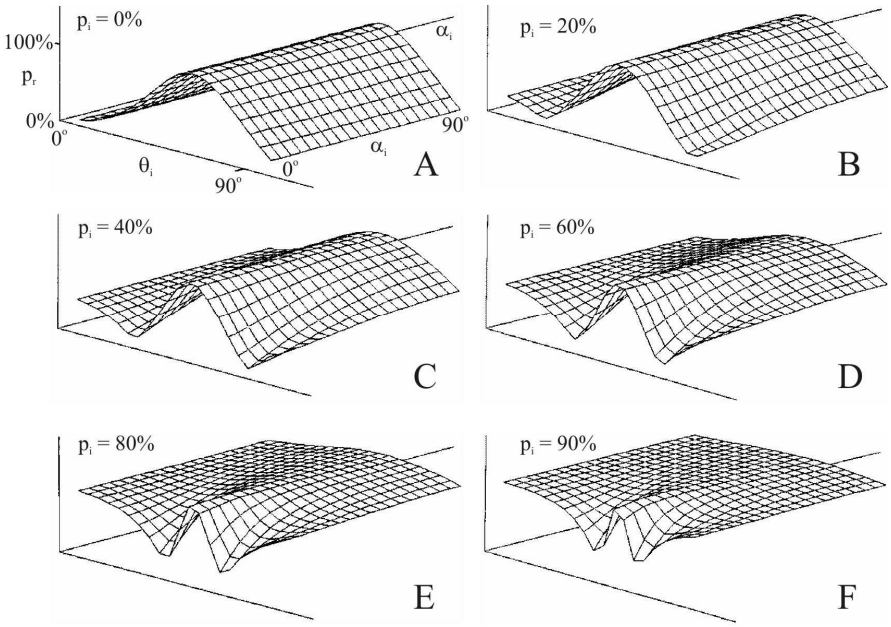

Fig. 11.4. Degree of linear polarization p_r of light reflected from the water surface as functions of the incident angle θ_i and angle of polarization α_i of partially linearly polarized incident light with six different p_i. (After Fig. 5.4 of Horváth 1993, p. 81).

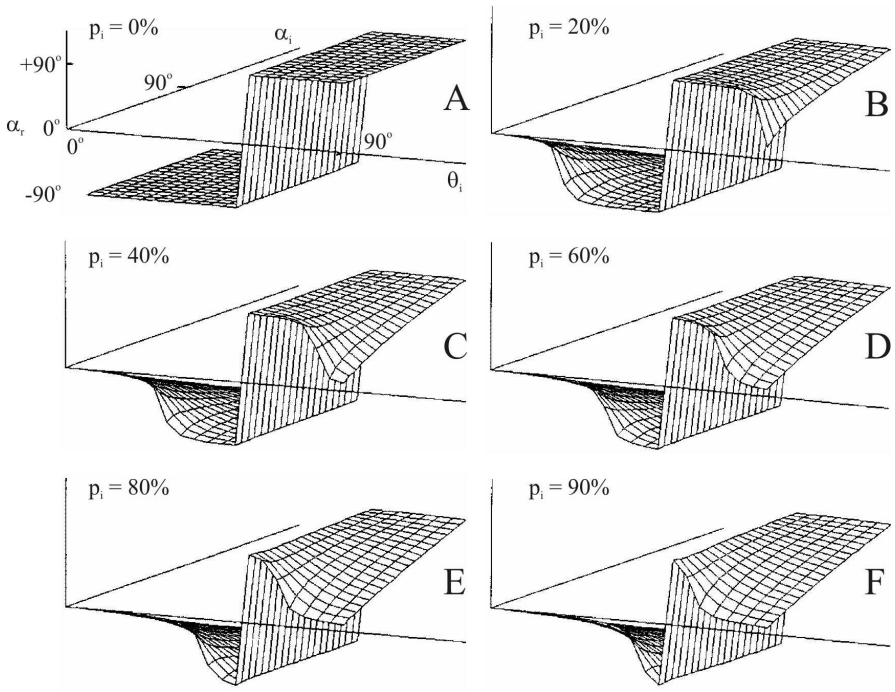

Fig. 11.5. Angle of polarization α_r of light reflected from the water surface as functions of the incident angle θ_i and angle of polarization α_i of partially linearly polarized incident light with six different p_i. (After Fig. 5.5 of Horváth 1993, p. 81).

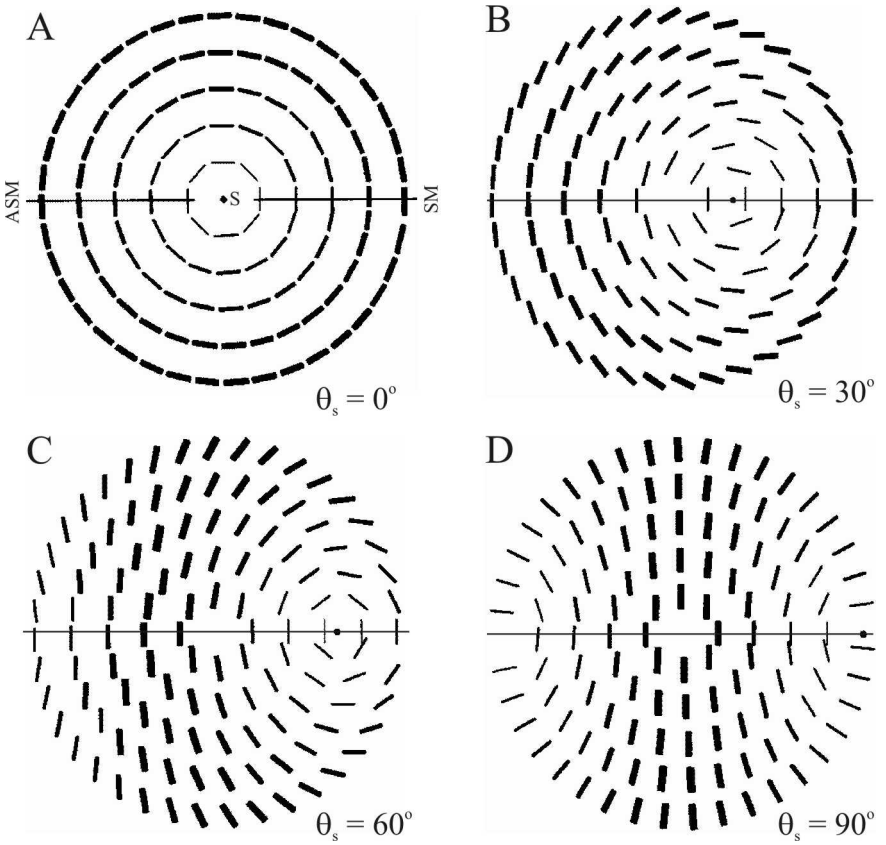

Fig. 11.6. Polarization pattern of the clear single-scattering Rayleigh sky for four different solar zenith angles θ_s. The alignment of the bars represents the direction of polarization and their width is proportional to the degree of linear polarization. The patterns represent the celestial hemisphere in two dimensions. The zenith is at the center, the position of the sun *S* is shown by a dot, the horizon is the outermost circle. ASM: antisolar meridian, SM: solar meridian. The zenith angle θ is measured radially (e.g. zenith: $\theta_z = 0^o$, horizon: $\theta_h = 90^o$) in such a way that the radius is proportional to θ. The azimuth angle φ is measured from the solar meridian (e.g. solar meridian: $\varphi_{SM} = 0^o$, antisolar meridian: $\varphi_{ASM} = 180^o$). (After Fig. 5.6 of Horváth 1993, p. 82).

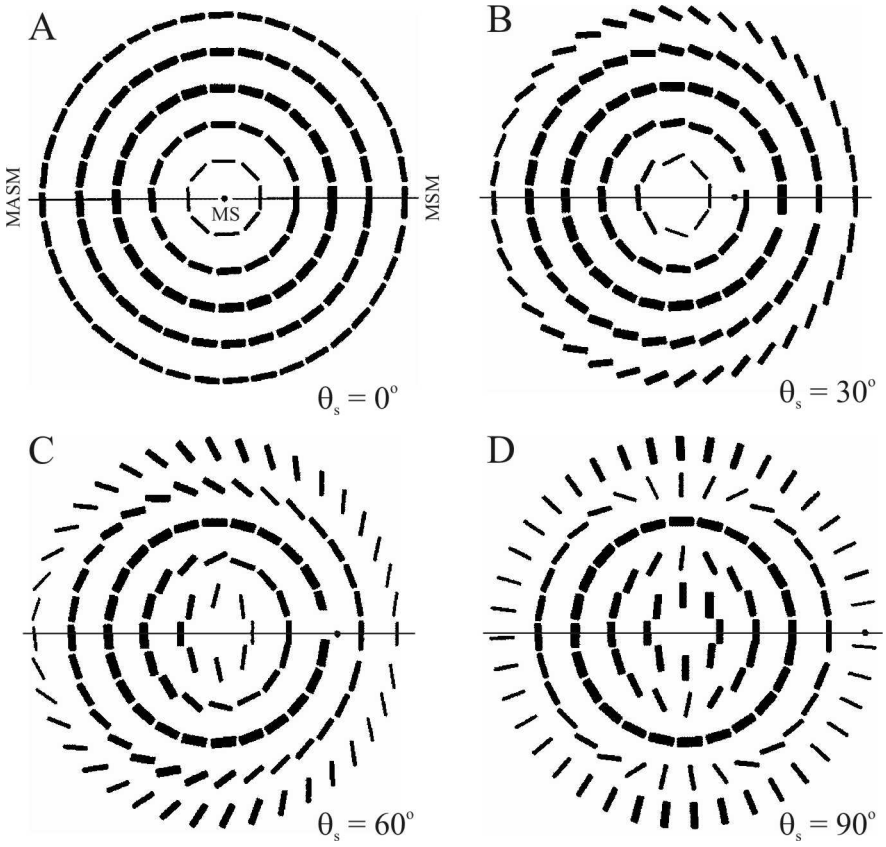

Fig. 11.7. As Fig. 11.6 for the reflection-polarization patterns of skylight at the flat water surface. MS: mirror sun, MSM: mirror solar meridian, MASM: mirror antisolar meridian. (After Fig. 5.7 of Horváth 1993, p. 83).

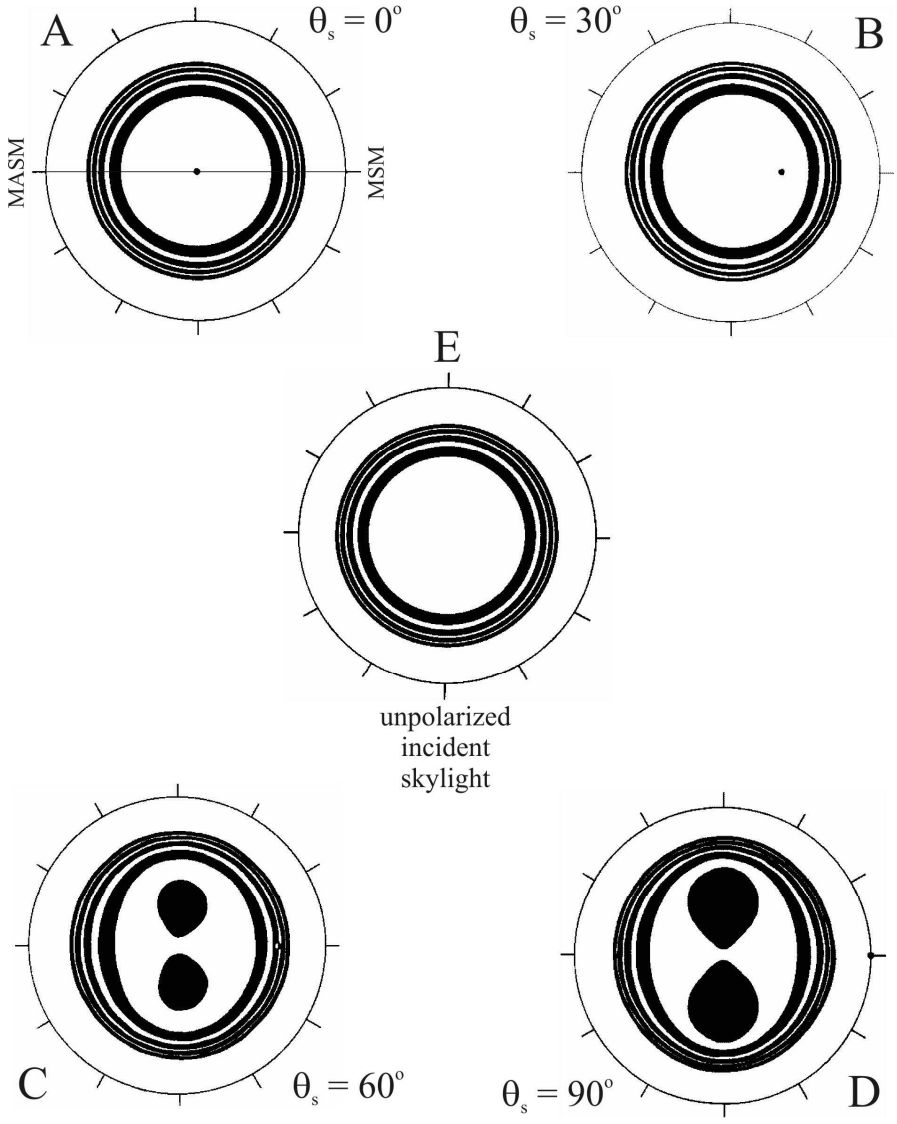

Fig. 11.8. Contour lines of equal reflectivity R for single-scattered Rayleigh skylight reflected from the water surface versus the solar zenith angle θ_s calculated for clear skies (A-D) and a totally clouded sky emitting unpolarized light (E). The positions of the sun are shown by dots. In patterns C and D the two central black spots represent the regions of the water surface where $R < 2\%$. In all patterns the elliptical or circular contour lines belong to $R = 3, 4, ..., 9, 10\%$ from the center towards the periphery, and the outermost circle at the horizon, with a graduation scale represents $R = 100\%$. For the sake of a better visualization every second reflectivity region is black. MSM: mirror solar meridian; MASM: mirror antisolar meridian. (After Fig. 5.10 of Horváth 1993, p. 87).

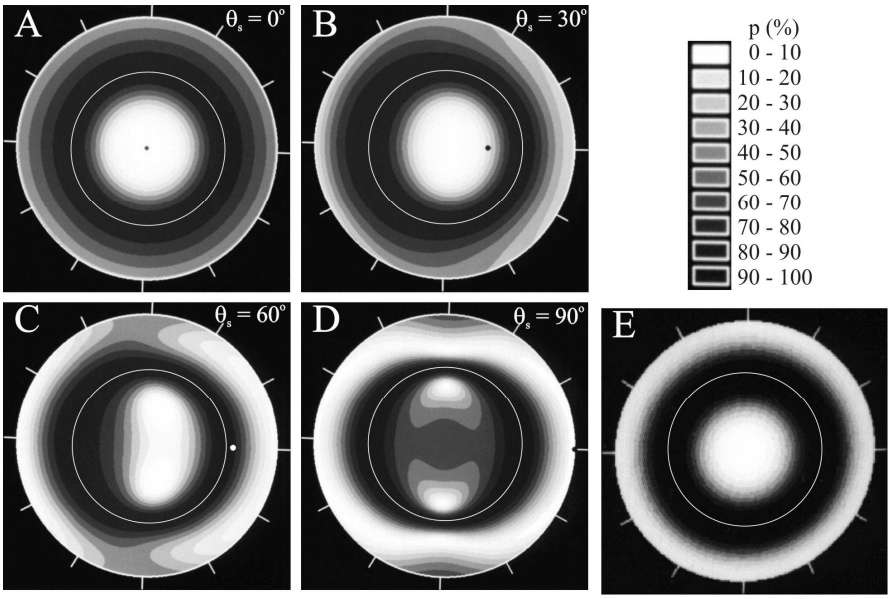

Fig. 11.9. A-D: Patterns of the degree of linear polarization p of light from the clear single-scattering Rayleigh sky reflected from the flat water surface for different solar zenith angles θ_s. The positions of the mirror sun are represented by dots. E: As A-D for unpolarized incident light from a totally cloudy sky. The white central circle in the strongly polarized annular zone in the patterns represents the Brewster angle $\theta_{Brewster} = 53^o$ from the vertical. (After Fig. 6.3 of Horváth 1993, p. 103).

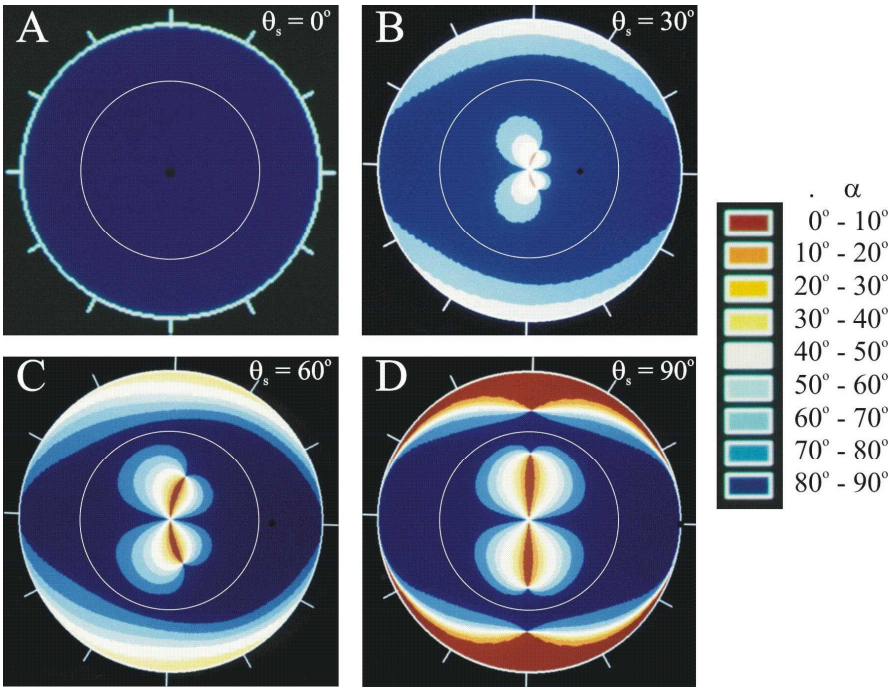

Fig. 11.10. As Fig. 11.9 for the angle of polarization α_r of reflected single-scattered Rayleigh skylight measured from the vertical. Since the E-vectors of skylight reflected from the water surface are horizontal when the sun is at the zenith, pattern A is homogeneously dark blue. (After Fig. 6.6 of Horváth 1993, p. 106).

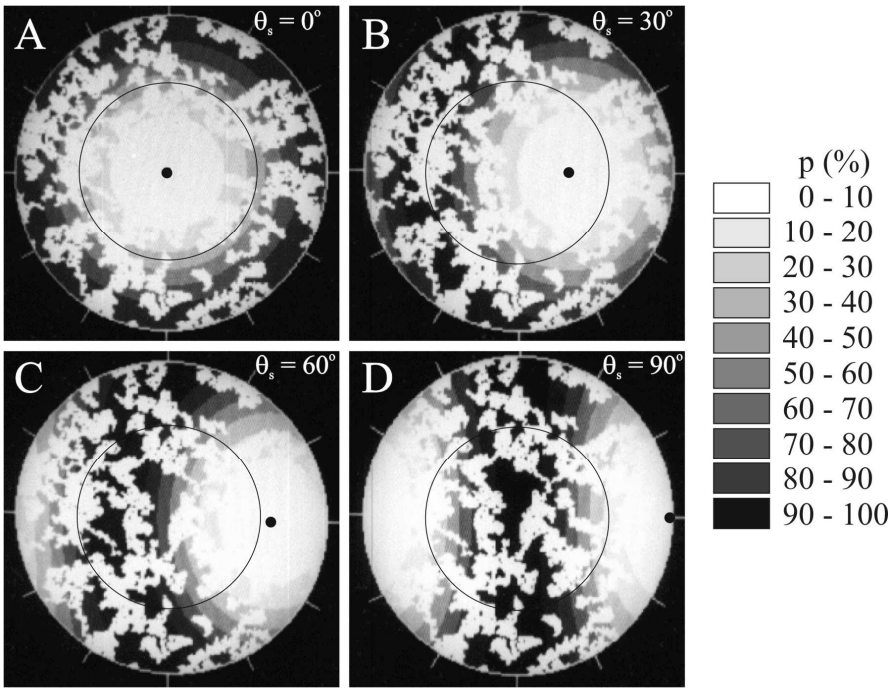

Fig. 11.11. Patterns of the degree of linear polarization p of light from the cloudy single-scattering Rayleigh sky for different solar zenith angles θ_s. The positions of the sun are represented by dots. The simulated clouds are white, because it was supposed that the light emitted by them is unpolarized (p = 0%). (After Fig. 6.2 of Horváth 1993, p. 102).

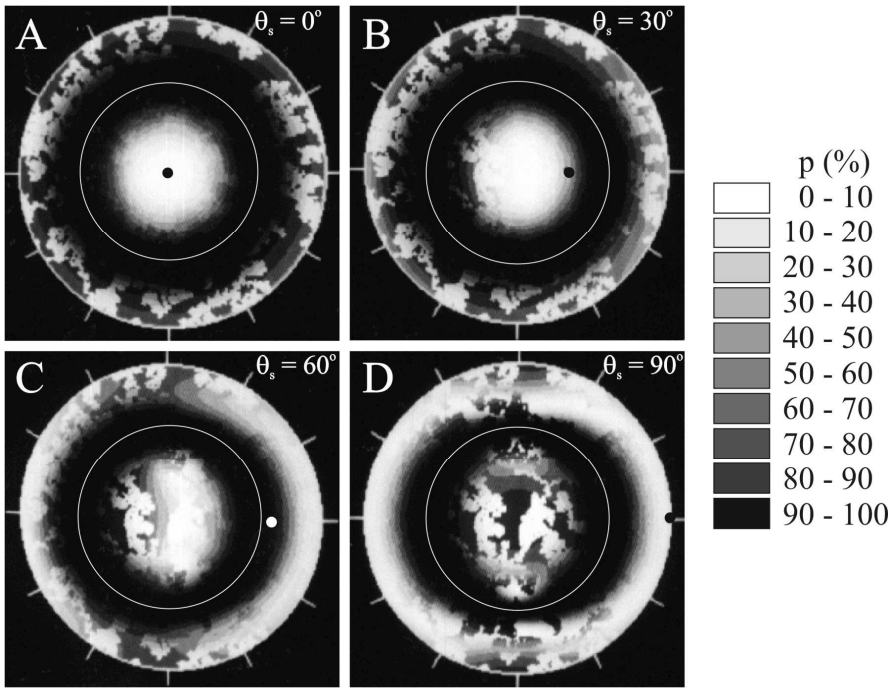

Fig. 11.12. As Figs. 11.9A-D with the same patterns of clouds as in Fig. 11.11. The mirror clouds visible at the smooth water surface are heterogeneously shaded by grey, because the unpolarized incident cloud light becomes horizontally polarized after reflection from the water surface with degree of polarization depending on the direction of view from the nadir as shown in Fig. 11.9E. (After Fig. 6.4 of Horváth 1993, p. 104).